Biochemical and Biophysical Research Communications 459 (2015) 113–117

Contents lists available at ScienceDirect

Biochemical and Biophysical Research Communications

journal homepage: www.elsevier.com/locate/ybbrc

Crystal structure of ATP-binding subunit of an ABC transporter from *Geobacillus kaustophilus*

M. Manjula [a], K.J. Pampa [b], S.M. Kumar [a], S. Mukherjee [c], N. Kunishima [d], K.S. Rangappa [e], N.K. Lokanath [a, *]

[a] Department of Studies in Physics, University of Mysore, Mysore 570 006, India
[b] Department of Studies in Microbiology, University of Mysore, Mysore 570 006, India
[c] Aurigene Discovery Technologies Ltd., #39/40, KIADB Industrial Area, Hosur Road, Electronic City Phase-II, Bangalore 560100, India
[d] Advanced Protein Crystallography Research Group, RIKEN SPring-8 Center, Harima Institute, 1-1-1 Kouto, Sayo-cho, Sayo-gun, Hyogo 679-5148, Japan
[e] Department of Studies in Chemistry, University of Mysore, Mysore 570 006, India

ARTICLE INFO

Article history:
Received 2 February 2015
Available online 25 February 2015

Keywords:
ATP binding protein
ABC transporter
Geobacillus kaustophilus
X-ray diffraction

ABSTRACT

The ATP binding cassette (ABC) transporters, represent one of the largest superfamilies of primary transporters, which are very essential for various biological functions. The crystal structure of ATP-binding subunit of an ABC transporter from *Geobacillus kaustophilus* has been determined at 1.77 Å resolution. The crystal structure revealed that the protomer has two thick arms, (arm I and II), which resemble 'L' shape. The ATP-binding pocket is located close to the end of arm I. ATP molecule is docked into the active site of the protein. The dimeric crystal structure of ATP-binding subunit of ABC transporter from *G. kaustophilus* has been compared with the previously reported crystal structure of ATP-binding subunit of ABC transporter from *Salmonella typhimurium*.

1. Introduction

Adenosine-5'-triphosphate (ATP) is an important molecule in cell biology and interacts with large number of proteins during biological reactions. ATP binding cassette (ABC) transporters, represent one of the largest superfamilies of primary transporters, which are very essential for various biological functions [1]. They are found in all phyla of life and are responsible for many physiological processes ranging from solute uptake to multidrug resistance. ABC transporters play a major role in nutrient uptake system, elimination of waste products, and resistance to antifungal agents, exporting cellular components which functions outside the plasma membrane and in an antibiotic production. ABC transporters couple hydrolysis of ATP to vectorial translocation of diverse substrates across cellular membranes [2]. The energy gained from ATP hydrolysis is utilized by the ABC transporters, for the purpose of transbilayer movement of substrates either into the cytoplasm (import) or out of the cytoplasm (export). Bacterial transporters are either export complex molecules (lipids, polysaccharides or proteins) or import small nutrients in cooperation with the soluble solute binding protein are also belongs to ABC transporters family. ABC transporters have a conserved domain structure and consist of two membrane-spanning domains that form the transport pathway and two cytosolic nucleotide-binding domains that energize the transport through the hydrolysis of ATP. The nucleotide-binding domains are highly conserved and contain an amino-acid sequence motif (LSGGQ) that is involved in the binding of nucleotides. This unique motif is known as C motif or signature motif [3].

Several structures of full-length ABC transporters (BtuCD from *Escherichia coli*, MsbA from *E. coli* and *Vibrio cholera*) and of many isolated nucleotide binding domains (NBDs), [HisP from *Salmonella typhimurium* [4], ABC transporter from *Methanococcus jannaschii* [5] and MalK from *E. coli* [6]] have been determined. The structures of NBDs are highly conserved, which include an ATP-binding core domain with Walker A and B motifs.

ATP-binding ABC transporters are abundant in biology, as they power the translocation of substrates across the membrane, often against a concentration gradient, by hydrolyzing ATP and have been subjected to biochemical and structural studies. In order to gain insight into the mechanism of ATP-binding subunit of an ABC transporter, we have initiated the structural studies of ATP-binding subunit of ABC transporter from *Geobacillus kaustophilus* (*Gka*ABC).

* Corresponding author.
E-mail address: lokanath@physics.uni-mysore.ac.in (N.K. Lokanath).

http://dx.doi.org/10.1016/j.bbrc.2015.02.079
0006-291X/

Table 1
Crystal data, data collection and refinement statistics of ATP binding subunit of ABC transporter from *Geobacillus kaustophilus*.

Data Collection statistics	
Space group	*I222*
Unit-cell parameters (Å, °)	$a = 54.94$, $b = 78.63$, $c = 112.96$
V_M (Å^3 Da^{-1})	2.32
Content of the asymmetric unit	Dimer
Resolution (Å)	50.0–1.77 (1.83–1.77)
Reflections (measured/unique)	166778/24183
R_{merge} (%)	5.3
Completeness (%)	99.9 (99.5)
$<I/\sigma(I)>$	18.8 (4.9)
Redundancy	6.9 (6.2)
Refinement statistics	
Resolution (Å)	50.00–1.77 (1.83–1.77)
R_{cryst} (%)	21.6
R_{free} (%)	25.0
rms bond lengths (Å)	0.005
rms bond angles (°)	1.24
Ramachandran plot (%)	
Most favored	96.64
Additional	1.68
Generous	1.68

Values in parentheses are for the highest resolution shell.

ATP-binding subunit of ABC transporter from *Gka*ABC, shows an amino-acid sequence identity of 26% to the ATP-binding subunit of ABC transporter from *S. typhimurium* (*Sty*ABC; HisP) [4]. We have reported the purification and crystallization of ATP-binding subunit of an ABC transporter from *G. kaustophilus* [7]. Here we report the high resolution crystal structure of ATP-binding subunit from *Gka*ABC, providing definitive evidence for the involvement of ATP binding in the molecular mechanism of ABC transporter.

2. Materials and methods

2.1. Protein purification and crystallization

The ATP-binding subunit of *Gka*ABC was purified and crystallized as described [7]. For the preparation of selenomethionine-substituted ATP-binding subunit of *Gka*ABC, the recombinant *E. coli* BL21 (DE3) Star (Invitrogen) cells were grown in M9 medium until they reached an absorbance at 600 nm (A600) of 0.4. At this point, 100 mg of L-lysine, 100 mg of L-phenylalanine, 100 mg of L-threonine, 50 mg of L-isoleucine, 50 mg of L-leucine and 60 mg of SeMet were added to 1 l of culture and the cells were grown at 37 °C for further 1 h, before inducing the expression with 1 mM IPTG overnight at 25 °C. The protein was purified using SuperQ Toyopearl 650, ResourceQ, Hydroxylapatite and Superdex 200 columns. The purified protein was concentrated to 12.2 mg/ml for crystallization studies. The selenomethionine-substituted ATP-binding subunit of *Gka*ABC was crystallized in a similar way as the native ATP-binding subunit of *Gka*ABC [7].

2.2. Data collection, structure determination and refinement

Data sets were collected at the synchrotron beam line BL26B1 at SPring-8, Japan, under cryogenic conditions. Crystals were flash-frozen with liquid nitrogen at 100 K in their respective mother liquor or soaking solution containing 25% (*v*/*v*) glycerol as

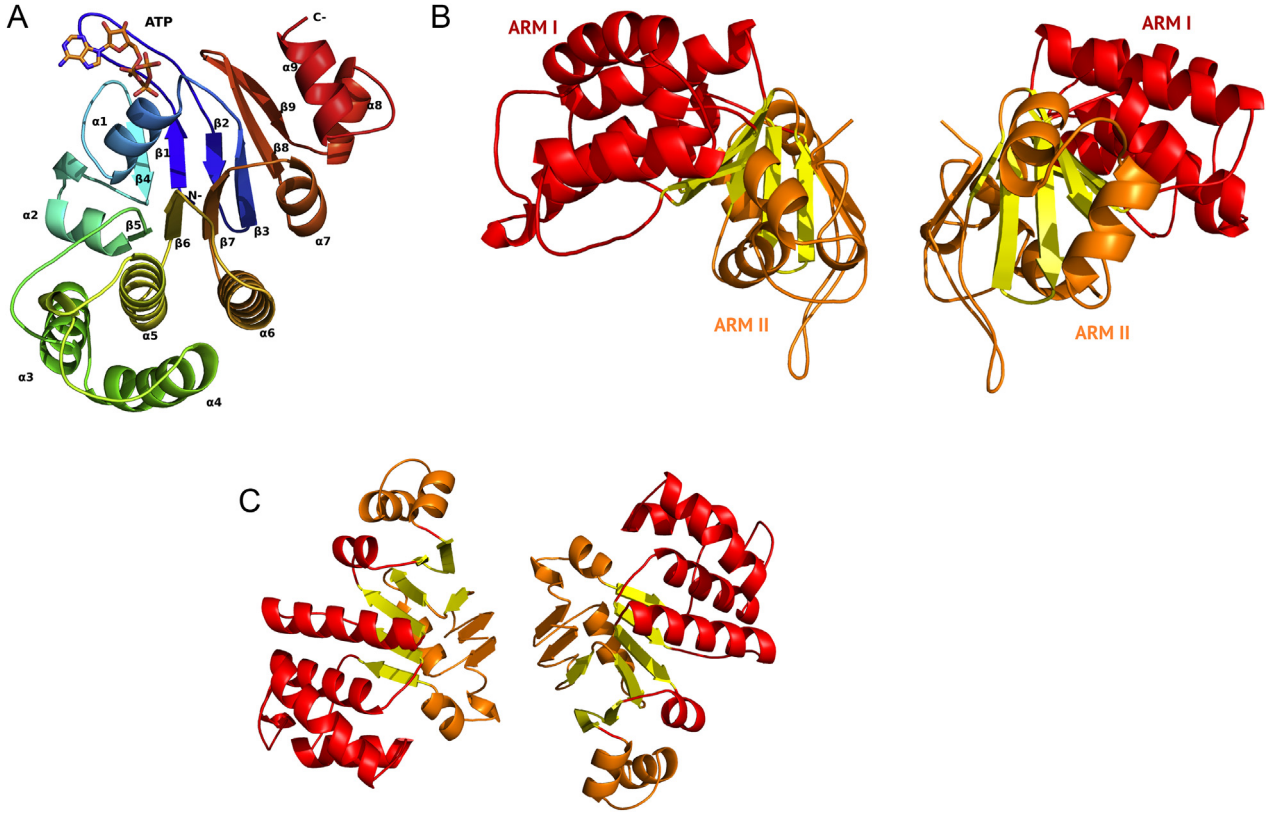

Fig. 1. Overall ribbon representation of ATP-binding subunit of *Gka*ABC. (A) The monomeric structure of ATP-binding subunit of *Gka*ABC, N-terminal and C-terminal are marked correspondingly. The docked ATP molecule is shown as ball-and-stick model. (B) View of the dimer along an axis perpendicular to its two-fold axis. Domains, arm I and arm II are represented by magenta and green colors. (C) Dimeric interface: The beta sheets β1, β2 and β4 are labeled at the dimer interface. (For interpretation of the references to color in this figure legend, the reader is referred to the web version of this article.)

cryoprotectant. The RIGAKU CCD detector was used for data collection. The data were processed and scaled using HKL 2000 suite [8]. The datasets were completed by including all possible *hkl* and R_{free} columns using UNIQUE of CCP4 suite [9]. The data collection parameters and processing statistics are given in Table 1.

The structure of ATP-binding subunit of *Gka*ABC was solved by multi-wavelength anomalous dispersion phasing method [10] using the automatic structure determination software SOLVE [11]. Refinement was carried out using CNS [12]. The model was further improved using the graphics program COOT [13] through its real space fitting and interactive manual building. Stereochemical quality of the coordinates was checked with the program PROCHECK [14]. The final atomic coordinates of ATP-binding subunit of *Gka*ABC are deposited in the RCSB Protein Data Bank (http://www.rcsb.org/pdb) with the accession codes 4RVC. The summary of the refinement statistics are given in Table 1.

2.3. Model analysis

DALI [15] server was utilized for structural similarity search against all known structures deposited in the protein data bank. Figures preparation and superposition of protein models were performed using PyMol (www.pymol.org). Dimeric surface area of ATP-binding subunit of *Gka*ABC and hydrogen bonds were calculated using PISA [16].

2.4. Molecular docking studies

Molecular docking analysis was performed using the docking programme Glide version 6.2 (Maestro. Schrodinger, USA). The atomic coordinates of ATP binding ABC transporter from *G. kaustophilus* was initially aligned with the HisP (PDB code 1B0U) coordinates employing protein structure alignment tool of Maestro 9.8 and then the ATP coordinates from 1B0U were transferred to 4RVC pdb. The resultant complex of 4RVC coordinates were minimized further through MacroModel 10.3 in a simulated aqueous environment, employing OPLS 2005 force-field, selectively constraining the protein and water coordinates. Docking grids were generated around the ATP binding site and the ATP from the complex was scored employing standard precision 'Score in Place' protocol of Glide 6.2. The images were prepared using PyMOL 1.0 [17].

3. Results and discussion

3.1. Overall structure of ATP-binding subunit of GKaABC

The crystal structure of ATP-binding subunit of *GKa*ABC had 245 amino-acid residues, of which we were able to model 241, we could not trace residues Asp242, Asp243, Ala244 and Pro245 in the electron-density map and thus not included in the final model. The ATP-binding subunit of ABC transporter belonged to α plus β class of protein folds with nine α–helices and nine β-strands, which are arranged as β1 – β2 – β3 – α1 - β4 – α2 - β5 – α3 – α4 – α5 – β6 - α6 -β7- α7 – β8 - β9 – α8 – α9 (Fig. 1A). These structures assembles into two domains (arm I and arm II) grouped together resembles 'L' shape (Fig. 1B). The arm I consists of a combination of α + β structures (β1-β2, β4, α1 and α2), whereas the arm II consists of only α helices (α3-α8) (Fig. 1B). In addition, the remaining beta sheets β3-β5-β6-β7-β8-β9 intermediates between the two arms.

Crystallographic analysis revealed that ATP-binding subunit of *Gka*ABC exists as apparent dimer in the crystal with extensive interface. These dimers (Fig. 1B) are consistent with the earlier studies on dynamic light-scattering showing the dimeric state of ATP-binding subunit of *Gka*ABC in solution [7] and the dimeric interface area is found to be 1022 Å^2. In the crystal structure,

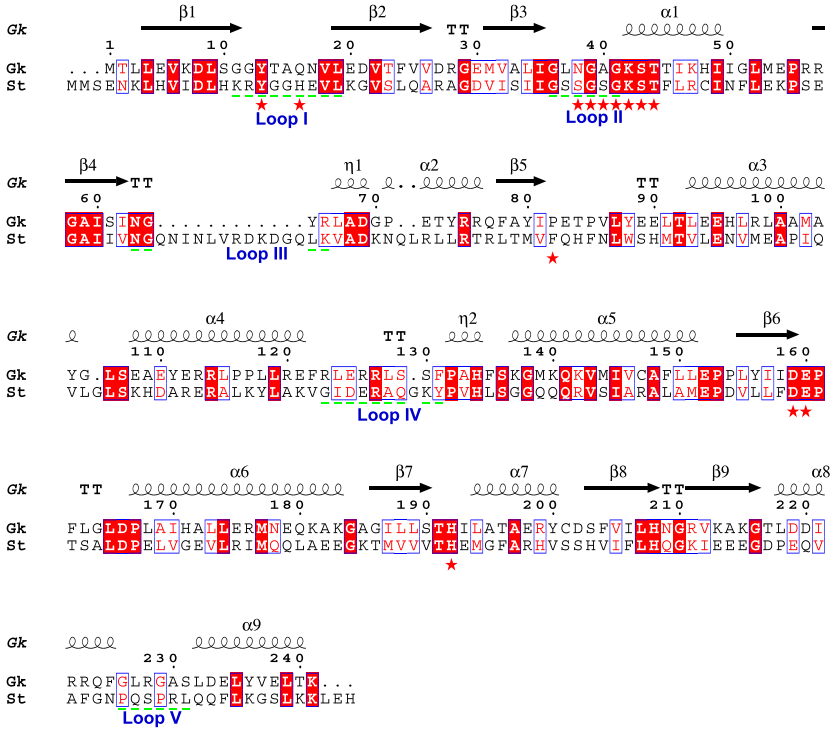

Fig. 2. Structure based sequence alignment of ATP binding subunit from *Gka*ABC and Histidine permase from *Salomonella typhimurium*. Red stars indicate residues involved in ATP binding. Green colored dashes represents the loops, and are labelled. Invariant residues are colored red. (For interpretation of the references to color in this figure legend, the reader is referred to the web version of this article.)

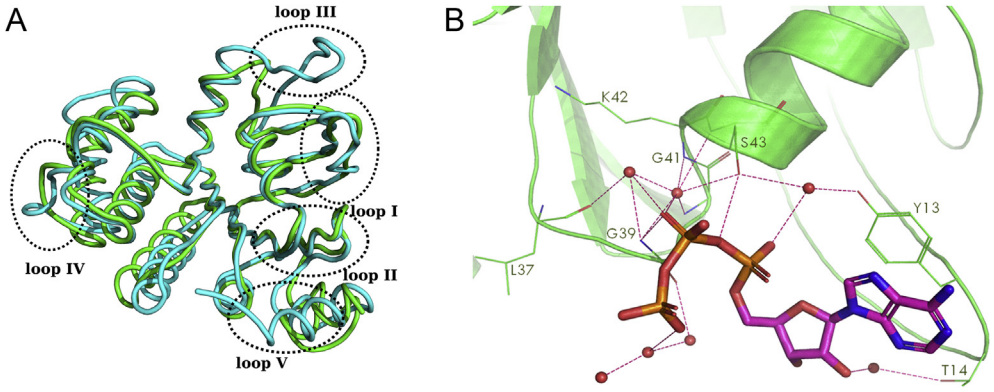

Fig. 3. (A) Superimposition of ATP binding subunit from *Gka*ABC and Histidine permease from *Sty*ABC subunit structures. ATP binding subunit from *Gka*ABC is colored in cyan and Histidine permease in green. Differences at the main-chain level between these two structures are circled with black broken lines. (B) Structural surroundings of ATP-binding subunit of ABC transporter. Docked ATP molecule is shown in ball-and-stick model, important residues are depicted as stick models and labeled, and water molecules shown in red spheres. Hydrogen bonds are indicated by broken lines (red). (For interpretation of the references to color in this figure legend, the reader is referred to the web version of this article.)

prtomer oligomerizes into dimer with major interactions from beta sheets (β1, β2 and β4) of the arm I (Fig. 1C). The invariant residue Asp8 located at the dimer interface is stabilized by intermolecular hydrogen bonds through water molecule. The residues (Gly39, Gly41, Lys42, Ser43 and Thr44) of phosphate binding loop within ATP binding pocket of arm I are conserved (Fig. 2). The invariant residues Asp159 and Glu160, which are important for ATP hydrolysis are located in the arm II.

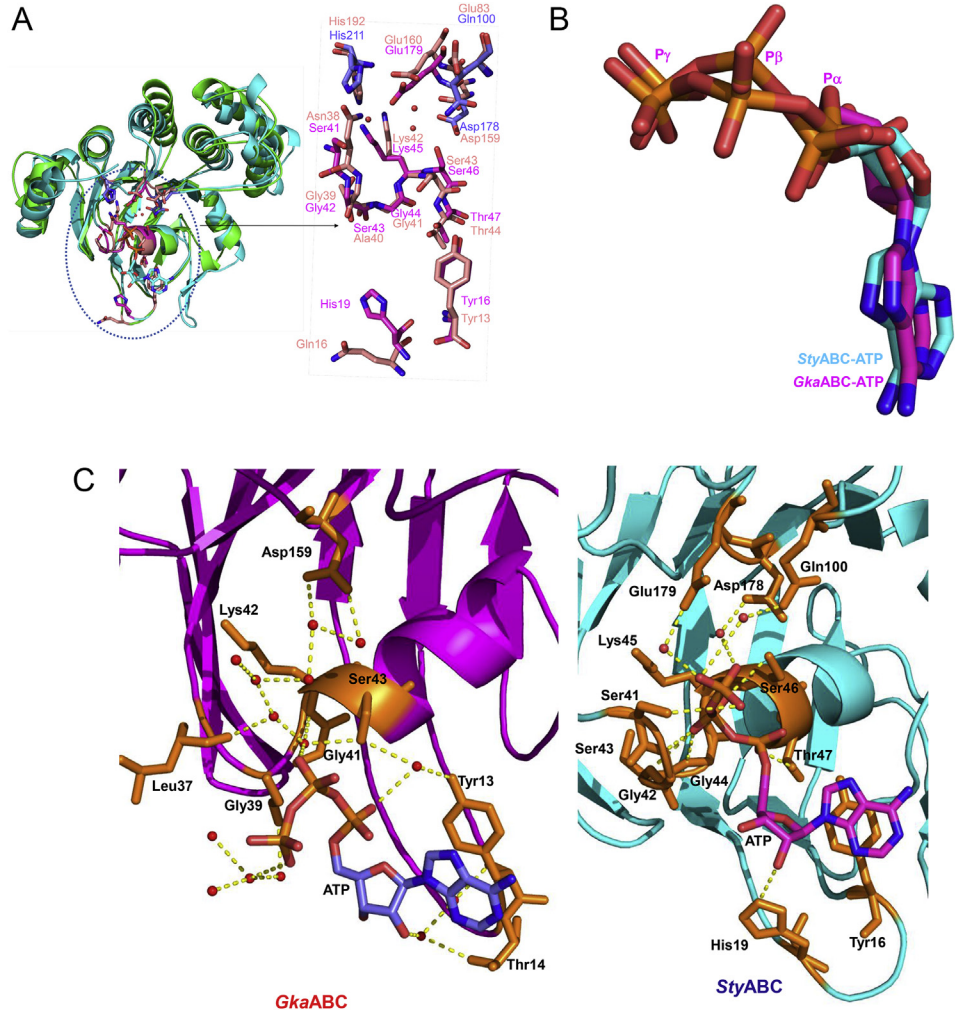

Fig. 4. Comparison of ATP-binding environment. (A) *Gka*ABC residues (ball-and-stick model) involved in the ATP binding (Tyr13, Gln16, Thr44, Asn38, Gly39, Ala40, Gly41, Lys42, Ser43, Thr44, Asp159, Glu160, His192 and Glu83) are compared with *Sty*ABC (Tyr16, His19, Ser41, Gly42, Ser43, Gly44, Lys45 and Glu179). The ATP molecule is shown as a stick model. (B) Superposition of ATP molecule of *Gka*ABC with *Sty*ABC. (C) Comparison of ATP-binding region of *Gka*ABC and *Sty*ABC. Structures of ATP-binding subunit of *Gka*ABC and *Sty*ABC are shown as cartoon diagram.

3.2. Structural comparison

The 3-D structural similarity search was performed using DALI server for ATP-binding subunit of *Gka*ABC coordinates with the available structures in the protein data bank. The closest structural homologue was found to be HisP, the ATP-binding subunit of the histidine permease (*Sty*ABC, PDB code 1B0U), which shared 26% of amino-acid sequence identity and shows a r.m.s.d of 1.347 Å for 169 Cα atoms on superposition (Figs. 2 and 3A) [4].

The overall structure of ATP-binding subunit of *Gka*ABC is similar to that of ATP-binding subunit of *Sty*ABC (HisP) [4]. However, structural divergences are found in the N-terminal region and loop regions (I, II, III, IV and V). The active site region is very well conserved. The structural differences have arisen in loops I, II, III, IV, and V due to deletion or insertion of amino acid residues (Fig. 3A). Three β-sheets of loops I, II and III are deleted and deletion of α-helix in the IV loop and V loop exhibits a significance deviation when compared to the structure of HisP (Fig. 3A). A conserved glutamine-rich sequence (LSGGQQQRV), termed as 'linker peptide' [18] or 'significant motif' [19] is evident. The overall structure of ATP-binding subunit of *Gka*ABC is well conserved with respect to functional and structural aspects, but with the exception of few loop regions [8].

3.3. ATP binding site and docking analysis

Attempt was made to co-crystallize ATP-binding subunit of *Gka*ABC with the ATP molecule but it failed to get ternary complex crystals. Therefore, docking analysis was performed to bind ATP molecule with the ATP-binding subunit of *Gka*ABC. Docking analysis was carried out to screen the potential active principle that could interact with the ATP molecule. The ATP molecule showed appreciable binding affinity and binding energy. The docked ATP molecule has better docking score of, -2.2. Residues, Tyr13 (side chain), Thr14 (side chain), Leu37 (back bone), Gly39 (back bone), Gly41 (back bone), Lys42 (back bone) and Ser43 (side chain) contribute to make hydrogen bonds with the ATP molecule (Fig. 3B). The 'phosphate-binding loop' or 'P-loop' which wraps the β-phosphate of ATP in ATP-binding pocket, has structures similar to that of nucleotide-binding proteins such as Ras and adenylate kinase [20]. This is analogous to the A motif of Walker's A/B motif [3].

The ATP binding environment of *Gka*ABC is similar to the ATP-binding of HisP (Fig. 4A). Binding of ATP molecules for both *Gka*ABC and *Sty*ABC protomers are superposed, and observed that adenine and ribose moieties are in the same conformation, whereas the tri-phosphate moiety shows a conformational deviation (Fig. 4B). The Pα-O2 directly hydrogen bonds to Thr44, Ser43 and through water molecule to Tyr13. Lys42 and Asp159 (with water molecule) interacts with oxygen of Pβ. Finally, oxygen atoms of Pγ hydrogen bonds to water molecules showing a conformation favorable to solvent roviding exposed (Fig. 4A and B).

The structural surroundings of the ATP binding region of ATP-binding subunit of *Gka*ABC are compared with ATP-binding of HiSP (Fig. 4A and B). The orange colored ball-and-stick residues represent the residues of *Gka*ABC and the residues of *Sty*ABC are represented by magenta and blue colored sticks. ATP binding residues are Tyr13 (Tyr16), Gln16 (His19), Thr44 (Thr47), Asn38 (Ser41), Gly39 (Gly42), Ala40 (Ser43), Gly41 (Gly44), Lys42 (Lys45), Ser43 (Ser36), Thr44 (Thr47), Asp159 (Asp178), Glu160 (Glu179), His192 (His211) and Glu83 (Gln100), where the residues within the paranthesis are from *Sty*ABC.

In conclusion, the high resolution crystal structure of ATP-binding subunit of *Gka*ABC has been determined. The apo-form structure of the ATP-binding subunit of *Gka*ABC is docked with ATP molecule. This structure is comparable to that of ATP-binding subunit of *Sty*ABC (HisP), which has similar properties. The active site, which provides the molecular basis for understanding the binding of ATP molecule, has been successfully identified.

Conflict of interest

None.

Acknowledgments

The authors would like to thank the UGC project (MRP-Phys-2013-32718), New Delhi for financial assistance and IOE single crystal X-ray diffraction facility, and DST-PURSE program, University of Mysore, Mysore. Authors would like to thank the beamline staff for assistance during data collection at beamline BL26B1 of SPring-8, Japan. M. Manjula thanks UGC-BRS for providing RFSMS fellowship.

References

[1] I.B. Holland, S.P.C. Cole, K. Kuchler, C.F. Higgins, ABC Proteins: from Bacteria to Man, Academic Press, London, UK, 2013.
[2] C.A. Doige, G.F.L. Ames, ATP-dependent transport systems in bacteria and humans: relevance to cystic fibrosis and multidrug resistance, Annu. Rev. Microbiol. 47 (1993) 291–319.
[3] J.E. Walker, M. Saraste, M.J. Runswick, N.J. Gay, Distantly related sequences in the alpha- and beta-subunits of ATP synthase, myosin, kinases and other ATP-requiring enzymes and a common nucleotide binding fold, EMBO J. 1 (1982) 945–951.
[4] L.W. Hung, X.W. Iris, N. Kishiko, Pei-Qi Liu, A. Giovanna Ferro-Luzzi, S.H. Kim, Crystal structure of the ATP-binding subunit of an ABC transporter, Nature 396 (1998) 703–707.
[5] N. Karpowich, O. Martsinkevich, L. Millen, Y.R. Yuan, P.L. Dai, K. MacVey, P.J. Thomas, J.F. Hunt, Crystal structures of the MJ1267 ATP binding cassette reveal an induced-fit effect at the ATPase active site of an ABC transporter, Structure 9 (2001) 571–586.
[6] J. Chen, G. Lu, J. Lin, A.L. Davidson, F.A. Quiocho, A tweezers-like motion of the ATP-binding cassette dimer in an ABC transport cycle, Mol. Cell. 12 (2003) 651–661.
[7] M. Manjula, K.J. Pampa, S. Madan Kumar, N. Kunishima, N.K. Lokanath, Purification, crystallization and preliminary X-ray diffraction studies of the ATP-binding subunit of an ABC transporter from *Geobacillus kaustophilus*, Acta Cryst. F68 (2012) 1406–1408.
[8] Z. Otwinowski, W. Minor, Processing of X-ray diffraction data collected in oscillation mode, Meth. Enzymol. 276 (1997) 307–326.
[9] Collaborative Computational Project, Number 4, The CCP4 suite: programs for protein crystallography, Acta Crystallogr. D. Biol. Crystallogr. 50 (1994) 760–763.
[10] W.A. Hendrickson, J.R. Horton, D.M. LeMaster, Selenomethionyl proteins produced for analysis by multiwavelength anomalous diffraction (MAD): a vehicle for direct determination of three-dimensional structure, EMBO. J. 9 (1990) 1665–1672.
[11] T.C. Terwilliger, J. Berendzen, Automated MAD and MIR structure solution, Acta Crystallogr. D. Biol. Crystallogr. 55 (1999) 849–861.
[12] A.T. Brunger, P.D. Adams, G.M. Clore, W.L. DeLano, P. Gross, R.W. Grosse Kunstleve, J.S. Jiang, J. wKuszewski, M. Nilges, N.S. Pannu, L.M. Rice, T. Simson, G.L. Warren, Crystallography & NMR System: a new software suite for macromolecular structure determination, Acta Crystallogr. D. Biol. Crystallogr. 54 (1998) 905–921.
[13] P. Emsley, K. Cowtan, Coot: model-building tools for molecular graphics, Acta Crystallogr. D60 (2004) 2126–2132.
[14] R.A. Laskowski, M.W. MacArthur, D.S. Moss, J.M. Thornton, PROCHECK: a program to check the stereochemical quality of protein structures, J. Appl. Cryst. 26 (1993) 283–291.
[15] L. Holm, C. Sander, Dali: a network tool for protein structure comaprision, Trends Biochem. Sci. 20 (1995) 478–480.
[16] E. Krissinel, K. Henrick, Detection of protein assemblies in crystals, in: Mrea Berhold (Ed.), Computational Life Sciences, Springer, Heidelberg Berlin, 2005, pp. 163–174.
[17] W.L. DeLano, The PyMOL Molecular Graphics System, DeLano Scientific, San Carlos, CA, USA, 2002.
[18] G.F. Ames, C. Mimura, S. Holbrook, V. Shyamala, Traffic ATPases: a superfamily of transport proteins operating from *Escherichia coli* to humans, Adv. Enzymol. 65 (1992) 1–47.
[19] M.A. Bianchet, Y.H. Ko, L.M. Amzel, P.L. Pedersen, Modeling of nucleotide binding domains of ABC transporter proteins based on a F1-ATPase/recA topology: structural model of the nucleotide binding domains of the cystic fibrosis transmembrane conductance regulator (CFTR), J. Bionerg. Biomemb 29 (1997) 503–524.
[20] E.F. Pai, W. Kabsch, U. Krengel, K.C. Holmes, J. John, A. Wittinghofer, Structure of the guanine-nucleotide-binding domain of the Ha-*ras* oncogene product p21 in the triphosphate conformation, Nature 341 (1989) 209–214.